JACS
JOURNAL OF THE AMERICAN CHEMICAL SOCIETY
Article
pubs.acs.org/JACS

Silver Nanoassemblies Constructed from Boranephosphonate DNA

Subhadeep Roy, Magdalena Olesiak, Shiying Shang, and Marvin H. Caruthers*

Department of Chemistry and Biochemistry, University of Colorado, Boulder, Colorado 80309, United States

Supporting Information

ABSTRACT: Spatially selective deposition of metal onto complex DNA assemblies is a promising approach for the preparation of metallic nanostructures with features that are smaller than what can be produced by top-down lithographic techniques. We have recently reported the ability of 2′-deoxyoligonucleotides containing boranephosphonate linkages (bpDNA) to reduce $AuCl_4^-$, Ag^+, and $PtCl_4^{2-}$ ions to the corresponding nanoparticles. Here we demonstrate incorporation of bpDNA oligomers into a two-dimensional DNA array comprised of tiles containing double crossover junctions. We further demonstrate the site-specific deposition of metallic silver onto this DNA structure which generates well-defined and preprogrammed arrays of silver nanoparticles. With this approach the size of the metallic features that can be produced is limited only by the underlying DNA template. These advances were enabled due to a new method for synthesizing bpDNA that uses a silyl protecting group on the DNA nucleobases during the solid-phase 2′-deoxyoligonucleotide synthesis.

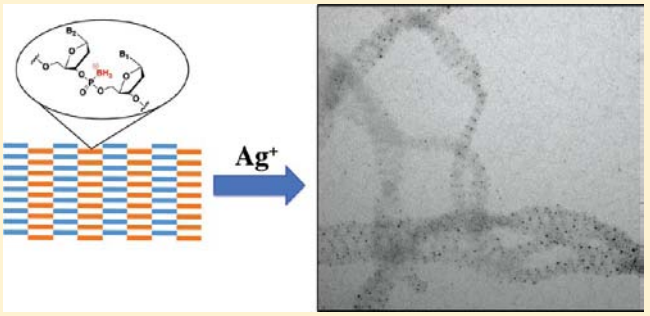

INTRODUCTION

The ability to manipulate and arrange matter in a preprogrammed manner at the nanoscale level lies at the crux of the bottom-up approach for creating functional materials. In particular, preparation of metallic nanostructures of a defined geometry leads to materials with optical and electronic properties that are expected to find applications as components of future electronics and optical devices.[1,2] A promising approach toward creating such well-defined assemblies of metal nanoparticles (NPs) having features smaller than what is possible using top-down technologies is based on the use of DNA as a scaffold.[3−5] DNA is well-suited for construction of nanostructures due to its programmable self-assembling properties, a well-defined and rigid secondary structure, and chemical stability to ambient conditions.[6−9] As a result of these favorable properties, increasingly complex two and three-dimensional (2D and 3D, respectively) DNA nanostructures have been realized.[10−23] In turn these developments have fostered efforts toward creating metal assemblies that use DNA nanostructures as templates.

DNA can be metallized by reduction of metal ions (Ag,[24−28] Au,[29,30] Pt,[31] Pd,[32,33] Ni,[34] and Co;[35] see ref 36 for a more exhaustive list of references) bound to the DNA backbone using exogenous agents, such as sodium borohydride or covalently attached aldehyde groups.[37−39] However these methods do not utilize the underlying addressability available within complex 2D and 3D DNA assemblies. Alternatively, gold nanoparticles (AuNPs) can be attached to thiol functionalized DNA. This allows site-specific immobilization of these particles at locations within a DNA assembly that contain a complementary sequence[40−52] Unfortunately the AuNPs in these experiments are negatively charged and cannot be placed any closer than 20−30 nm due to interparticle repulsions.[52,53] This constrains the size, complexity, and density of metallic features that can be produced even though the available 'pixel size' in underlying DNA structures can be as small as 3 × 7 nm.[23]

We recently reported that DNA containing boranephosphonate internucleotide linkages (bpDNA), as shown in Figure 1, reduce many metal ions ($AuCl_4^-$, $PtCl_4^{2-}$, and Ag^+) and produce the corresponding NPs.[54] At the same time, previous research has demonstrated that bpDNA forms standard Watson−Crick base pairs.[55−58] Thus the programmable Watson−Crick binding properties can be used to incorporate bpDNA at predetermined sites within a DNA structure, while the reductive group will lead to metal deposition at these sites upon exposure to metal salts. In the example outlined in Figure 1, only one of the two alternating tiles (shown as orange in this example) that comprise this particular DNA array is programmed to contain bpDNA (see also Figure 4). When this array is exposed to a metallic salt, metal particles, as illustrated by the golden colored spheres, will be deposited selectively at the orange tiles to form a preprogrammed, linear arrangement of NPs. Moreover because the concentration and spatial distribution of the reductive boranephosphonate linkages can be freely varied even within the same bpDNA, a high degree of control over the size and density of the metallic features may be achieved.

In spite of these promising attributes, the use of bpDNA for constructing metal-NP assemblies has not been realized. This is because none of the synthetic approaches reported pre-

Received: January 26, 2013
Published: April 4, 2013

   dx.doi.org/10.1021/ja400898s | J. Am. Chem. Soc. 2013, 135, 6234−6241

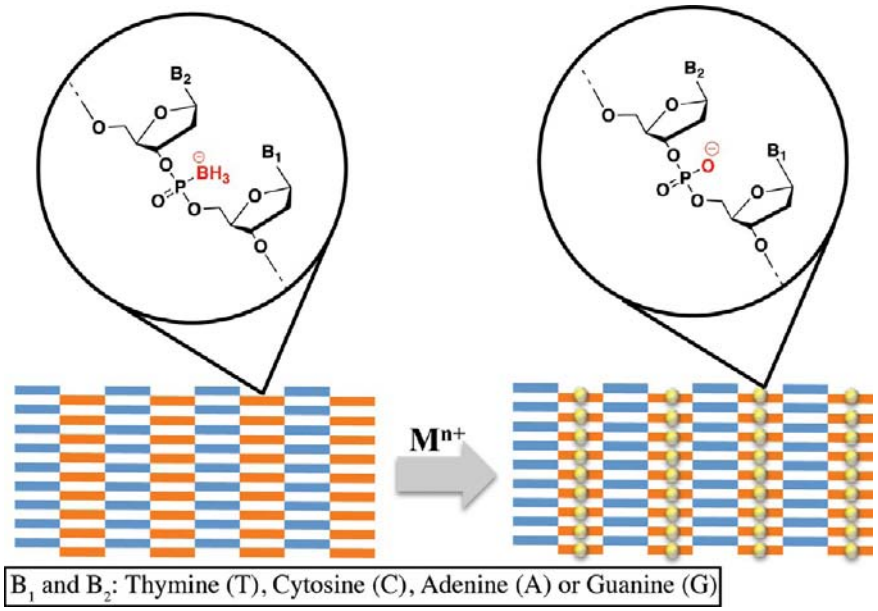

Figure 1. Schematic depiction of selective metal deposition by controlling the location of bpDNA. In this example only the orange tiles contain bpDNA. Metal deposition (golden yellow spheres) occurs at the orange tiles when the preassembled array is exposed to a metal salt. The boranephosphonate linkage is oxidized to a phosphate without degradation of the backbone during this process.[54]

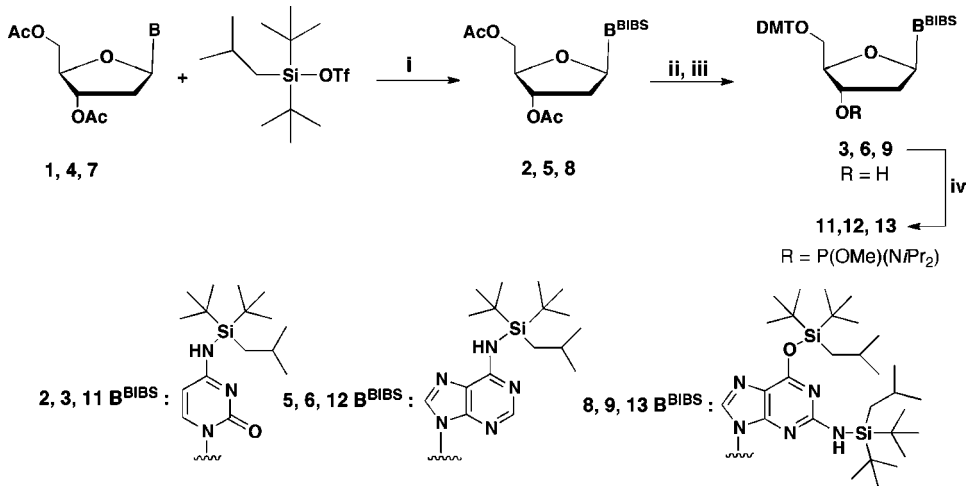

Figure 2. Synthesis of BIBS protected 2′-deoxynucleoside 3′-phosphoramidites. (i) Et_3N, DMAP and 1,4-dioxane; (ii) 1.0 M NH_3/MeOH; (iii) DMT-Cl (1.2 equiv), diisopropylethylamine (2 equiv), pyridine; and (iv) $P(OMe)(NiPr_2)_2$ (1.2 equiv), tetrazole (1.1 equiv), and CH_2Cl_2.

viously[59−64] can be used to synthesize bpDNA of sufficient length and purity necessary for nanotechnology applications. In this report, we present a new synthetic method that overcomes these limitations. We demonstrate incorporation of bpDNA into a 2D DNA nanoarray comprised of tiles containing double crossover (DX) junctions.[63] This particular type of tile was chosen as a large number of DNA assemblies including addressable 2D arrays[23] and origami structures contain these DX motifs. We last demonstrate site-specific, *in situ* deposition onto these arrays of silver nanoparticles (AgNPs) simply by treating with solutions containing Ag^+.

RESULTS

Synthesis of *N*-BIBS Protected 2′-Deoxynucleoside 3′-Phosphoramidites. The synthesis of bpDNA is problematic due to reduction of the amide groups that protect the nucleobase exocyclic amines of adenine, guanine, and cytosine during DNA synthesis.[60] This reduction is caused by the borane reagents used to generate the boranephosphonate linkages. Thus our challenge lay in developing a new type of protecting group that was stable to borane as well as other reagents used during 2′-deoxyoligonucleotide synthesis. Recently Liang et al[66] reported the protection of amines using the di-*tert*-butylisobutylsilyl (BIBS) group. In contrast to the lability of amines protected with nonhindered silanes,[67,68] the BIBS group was shown to be quite stable. In addition no reactivity towards borane was expected *a priori*. Thus we sought to develop a synthetic scheme for preparing BIBS protected 2′-deoxynucleoside 3′-phosphoramidites that could be used as synthons for DNA and bpDNA synthesis.

Figure 2 depicts the synthetic scheme that was developed for the preparation of BIBS protected 2′-deoxynucleoside 3′-phosphoramidites. Starting with 5′,3′-di-*O*-acetyl 2′-deoxynucleosides (**1**, **4**, or **7**), silylation of the exocyclic amines was carried out using variations of the reported procedure.[65] The reaction of 5′,3′-di-*O*-acetyl-2′-deoxycytidine (**1**) with BIBS-

dx.doi.org/10.1021/ja400898s | *J. Am. Chem. Soc.* 2013, 135, 6234−6241

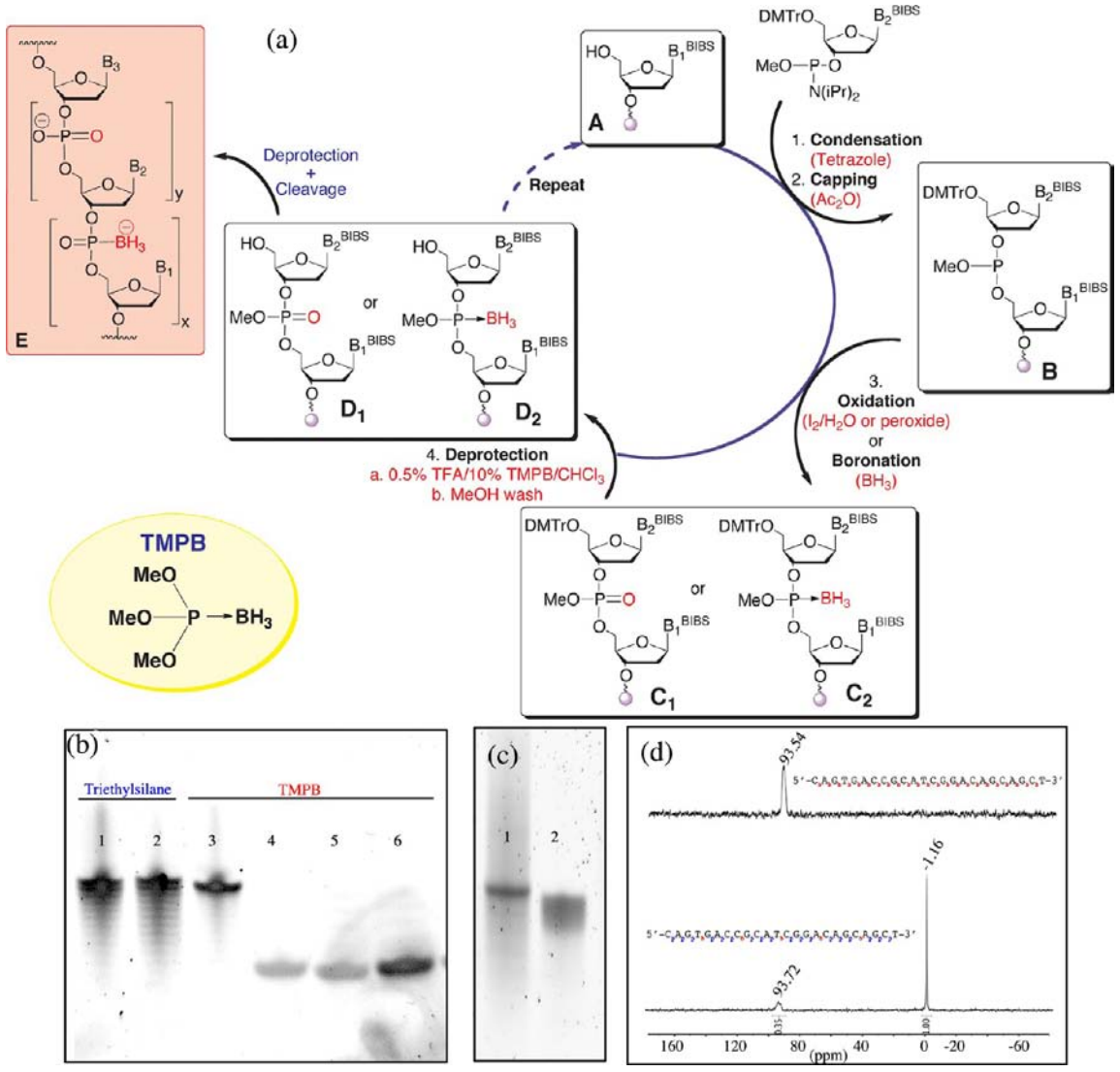

Figure 3. (a) Synthetic cycle for DNA and bpDNA synthesis using BIBS protected phosphoramidites. (b) Lanes 1 and 2: **bpdT$_{21}$** synthesized using Et_3SiH as scavenger. This mixture was found to contain many degradation products. Lane 3: **bpdT$_{21}$** synthesized using TMPB as a trityl scavenger. 5′-*O*-DMT-2′deoxythymidine 3′-*O*-cyanoethyl *N*,*N*-diisopropylaminophosphoramidite was used for results shown in lane 1, whereas 5′-*O*-DMT-2′-deoxythymidine 3′-*O*-methyl *N*,*N*-diisopropylaminophosphoramidite was used for results displayed in lanes 2 and 3. Lanes 4−6: Reactions mixtures obtained from the synthesis of **bpd(T$_8$CT)**, **bpd(T$_8$AT)**, and **bpd(T$_8$GT)**, respectively, using BIBS protected phosphoramidites and TMPB as a scavenger. (c) Denatuing PAGE analysis of reaction mixtures obtained from the synthesis of mixed based sequences **bpdB1a** (lane 1) and **3−1bpdB1a** (lane 2). (d) ^{31}P NMR spectra of purified **bpdB1a** (top) and **3−1bpdB1a** (bottom). Sequences of **bpdB1a** and **3−1bpdB1a** are shown in Figure 3d. Subscript 'p' and 'b' refer to a phosphate and boranephosphonate linkages, respectively.

OTf (Tf = triflate) in the presence of base proceeded in 2 h at 50 °C with good yield (67%), whereas 5′,3′-di-*O*-acetyl-2′-deoxyadenosine (**4**) reacted more slowly and required heating at 60 °C for 3 days in order to obtain the product in 25−30% yield. These results are in accordance with the lower nucleophilicity of the adenine amine. Use of stronger bases, prolonged reactions times, and higher temperatures (80 °C) did not improve yields. The reaction of 5′,3′-di-*O*-acetyl 2′-deoxyguanosine (**7**) with 1.2 equiv of BIBS-OTf (60 °C) led to substitution at the O^6 position instead of the N^2 amine (Scheme S1 and Figure S4). However when repeated with a larger excess (5 equiv) of BIBS-OTf (60 °C) for 3 days, the bis(silyl) compound (**8**) was obtained in 74% yield.

Removal of the 5′ and 3′ acetyl groups on **2**, **5**, and **8** with 1.0 M ammonia in methanol was followed by protection of the 5′ hydroxyl as the dimethoxytrityl (DMT) ether to yield **3**, **6**, and **9**. Finally, the 3′ hydroxyl was phosphitylated using O-methyl-bis(*N*,*N*-diisopropylamino)phosphoramidite activated by tetrazole to yield synthons **11**−**13** in good yields (85−95%).

bpDNA Synthesis using BIBS-Phosphoramidites and a Novel Trityl Quencher. Solid-phase DNA synthesis using the phosphoramidite method is comprised of four steps, as shown in Figure 3a. For bpDNA synthesis, the oxidation (step 3) of the phosphite triester to phosphate (**C1**) with peroxide or iodine is replaced by boronation with BH_3 to yield a trialkylphosphite borane linkage (**C2**). Since no examples of *N*-silyl nucleobase protecting groups for DNA synthesis exist, we sought to determine the stability of the BIBS groups during solid-phase 2′-deoxyoligonucleotide synthesis by preparing DNA containing only phosphate diester internucleotide linkages. These experiments demonstrated that **12** and **13** could be used without modification of the standard conditions

dx.doi.org/10.1021/ja400898s | J. Am. Chem. Soc. 2013, 135, 6234−6241

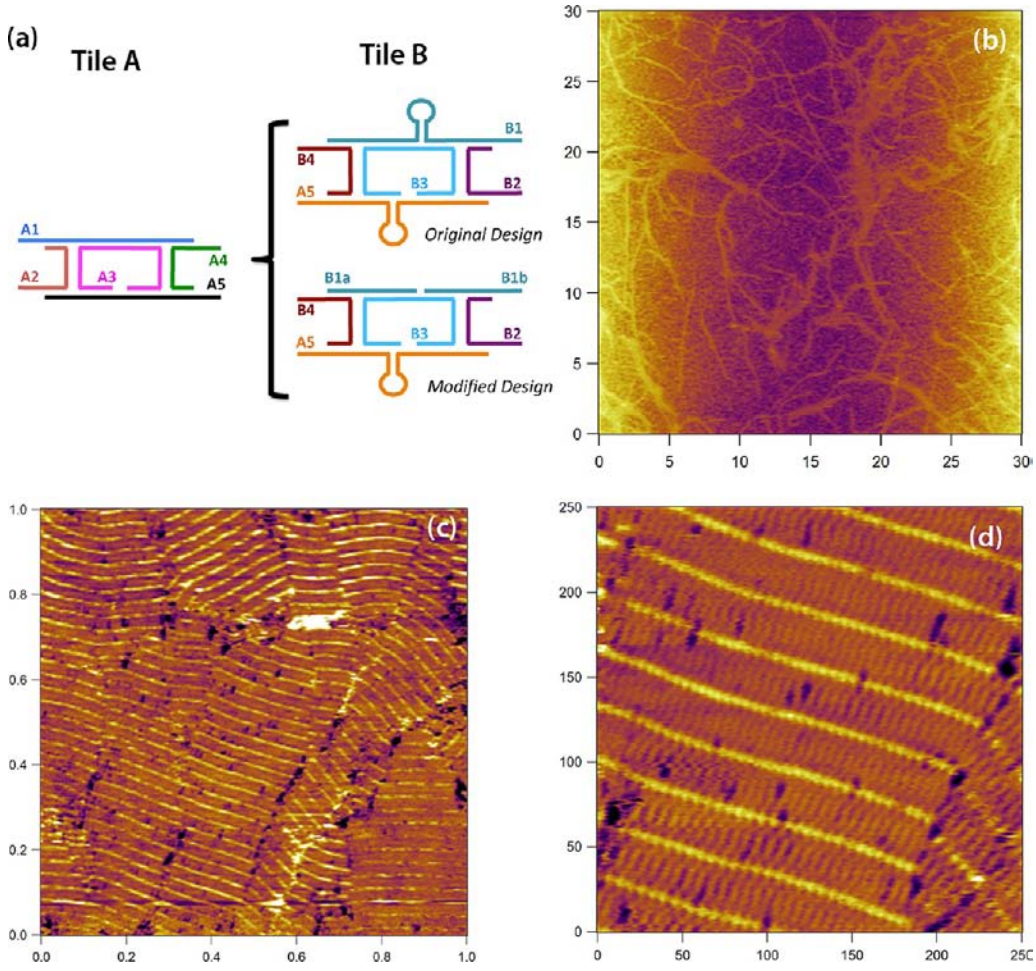

Figure 4. (a) Modified design of Tile B for incorporation of bpDNA. (b–d) AFM images of 2D arrays that incorporate the fully boronated B1a (**bpB1a**) in the modified design. The $x-y$ scale for images displayed in (b) and (c) are in μm, while the image in (d) is in nm. The stripes at higher magnification result from the rows of vertical hairpin loops present in modified tile B.

(data not shown). However for **11** the 3% trichloroacetic acid (TCA) in dichloromethane solution, which is routinely used for detritylation, led to partial removal of the BIBS group during each synthesis cycle (Figure S5a and S6). Further studies also revealed that this effect was specific to TCA as BIBS removal was not observed when a 0.5% trifluoroacetic acid (TFA) solution (Figure S5b) was used. It is known that TCA binds strongly to 2′-deoxyoligonucleotides on a solid support,[69] which leads to a high local concentration of acid. Perhaps this increased acid concentration causes an enhanced rate of acid-mediated BIBS cleavage. In contrast TFA likely does not interact similarly with the 2′-deoxyoligonucleotides. Irrespective of the rational, substitution of TFA in the detritylation step (Figure 3a, step 4) led to the preparation of several DNA oligomers in high yield and purity (Figures S7 and S8 and Table S2).

A second challenge that must be addressed for the successful synthesis of bpDNA stems from the reaction of trityl cations, generated in step 4 (Figure 3a), with the trialkyl phosphite borane linked bpDNA (**C2**). This reaction degrades the growing 2′-deoxyoligonucleotide chain.[60,70,71] Although triethylsilane has been described as an efficient trityl cation scavenger,[63] the synthesis of a fully boronated 2′-deoxythymidine 21-mer, (**bpdT**$_{21}$; Table S3) using an acid deprotection mixture containing 50% (v/v) Et_3SiH, led to significant amounts of shorter length products (Figure 3b, lanes 1 and 2). We therefore reasoned that an analog of the trialkylphosphite-borane internucleotide linkage as found in **C2** (Figure 3a) would be a more effective quencher. Accordingly bpDNAs **bpdT**$_{21}$, **bpd**(**T**$_8$**AT**), **bpd**(**T**$_8$**CT**), and **bpd**(**T**$_8$**GT**) were synthesized using 10% (v/v) trimethylphosphite-borane (TMPB; Figure 3a) as the trityl scavenger in 0.5% TFA/$CHCl_3$. Denaturing PAGE analysis of these reaction mixtures showed the formation of single bands (Figure 3b, lanes 3–6) for each oligomer. MALDI-TOF analysis after elution from the gel confirmed synthesis of the expected products (Table S3).

In order to more thoroughly test this synthesis method, two 24-mer boranephosphonate DNAs (**bpdB1a** and **3–1bpdB1a**) that contained all four 2′-deoxynucleosides were synthesized (see Figure 3d for the sequences of these bpDNAs). **bpdB1a** was boronated at every internucleotide linkage, whereas **3–1bpdB1a** contained an alternating pattern of three phosphates and one boranephosphonate. For **3–1bpdB1a**, the phosphite triester produced after the coupling step (Figure 3a; compound **B**) was either oxidized to phosphate (**C1**, Figure 3a) with 1.0 M *tert*-butyl hydroperoxide in CH_2Cl_2 or to boranephosphonate (**C2**, Figure 3a) using a BH_3/THF complex. All other conditions remained the same. Denaturing PAGE analysis of the reaction mixture obtained from the synthesis of **bpdB1a** revealed a single product (Figure 3c, lane 1). However in the case of **3–1bpdB1a** (Figure 3c, lane 2) a more diffuse band, which indicates the presence of failure products, was observed.

dx.doi.org/10.1021/ja400898s | J. Am. Chem. Soc. 2013, 135, 6234–6241

These are likely due to incomplete oxidation as *t*-BuOOH is known to be less efficient than iodine as an oxidant (iodine leads to degradation of compound **C2** and cannot be used for synthesis of DNA containing boranephosphonate and phosphate linkages). Nevertheless both bpDNAs were purified by preparative gel electrophoresis and confirmed to be the correct product by MALDI-TOF MS (Table S3) and ^{31}P NMR (Figure 3d). Thus by using a combination of BIBS protected phosphoramidites, TFA for detritylation, and TMPB as a trityl cation scavenger, mixed sequence bpDNAs of lengths far greater than previously possible could be synthesized.

Incorporation of bpDNA into 2D DNA Arrays. Winfree et al.[10] were the first to describe the use of rigid DNA tiles containing DX junctions for the assembly of 2D DNA lattices. This DX motif has continued to be used in a number of DNA nanostructures, including various origami-based assemblies[72] as well as complex and addressable 2D shapes.[23] Because of the many potential applications of this motif, we chose Winfree et al's 2D arrays as a test system for incorporation of bpDNA into DNA-based assemblies. Also incorporation of bpDNA within one of the alternating tiles would be expected to produce a predictable pattern of metal NPs upon *in situ* reduction of Ag^+ ions.

The original design[10] contained two alternating tiles (tiles A and B; Figure 4a). Each tile in turn was comprised of five individual DNA sequences (A1−A5 and B1−B5). Upon assembly, each DX tile displayed complementary sticky ends on the corners which generates intertile contacts. This design therefore allowed the formation of arrays with an alternating pattern of tiles. The B1 and B5 sequences of tile B also contained vertical hairpin loops as topographical markers for AFM experiments. In order to incorporate bpDNA, the hairpin loop segment on B1 was deleted, and the resultant strand was divided into two individual oligomers that were 24 and 23 nucleotides in length (B1a and B1b, respectively). Fully (**bpdB1a**) and partially (**3−1bpdB1a**) boronated versions of B1a were synthesized (Table S3). Such a split design was necessary because attempts to synthesize the entire B1 sequence (47 nucleotides without the hairpin loop) as a fully boronated bpDNA yielded a hydrophobic material that was insoluble in aqueous solution and could not be characterized. Boranephosphonates are more lipophilic than phosphates,[55] and therefore the hydrophobic nature of this bpDNA oligomer was not surprising. Although it was possible to synthesize the 47-mer B1 strand as a phosphate-boranephosphonate oligomer, the expected lower yields for such an oligomer (for instance see gel pattern for **3−1bpdB1a** which is 24 nucleotides in length) dissuaded us from doing so.

For assembling the 2D arrays, 1 bpDNA and 10 DNA strands were mixed together in a 20 mM tris-acetate (pH 7.4) buffer containing 10 mM $Mg(OAc)_2$. The arrays were annealed by cooling the mixture from 94 °C to room temperature over 2 days in a 2 L water bath. AFM analysis of the annealed structure (Figure 4b−d) revealed large, flat arrays that were several micrometers in length and a few hundred nanometers in width. An average spacing of 31 ± 1 nm between the rows of hairpin loops was obtained which is in good agreement with an expected value of 33 nm. As a negative control we also annealed a solution where all the strands except **bpdB1a** were included. When examined by AFM, no arrays were observed which confirms the requirement for the **bpdB1a** strand in order to successfully assemble this 2D array. The rigid DX tiles are known to be highly sensitive to the structure of the constituent double helices, and deviations from the B-form helical parameters can lead to failure of structure formation. However our results show that the introduction of boranephosphonates that contain a chiral P atom was well-tolerated, and no discernible effect on formation of arrays was observed. Arrays of similar quality were also produced with the **3−1bpdB1a** oligomer (Figure S9).

In situ Metallization of bpDNA Containing Arrays. In order to produce assemblies of AgNPs, we first deposited the DNA arrays that incorporated the **bpdB1a** strand on transmission electron microscopy (TEM) grids. The arrays were subsequently treated with a 20 mM tris-acetate buffer (pH 7.4) containing 0.5 mM $AgNO_3$ and 10 mM $Mg(OAc)_2$ (20 h in a humidity chamber). Excess liquid was removed, and the grids were washed three times with water. Deposition of metal NPs at the sites containing bpDNA was expected to produce a striped pattern of AgNPs. In addition previous reports have shown that deposition of NPs can cause these flat arrays to roll up into tubular structures.[43,47] Consistent with these expectations, transmission electron micrographs of these metalized, bpDNA containing arrays (Figure 5 and S11) demonstrated

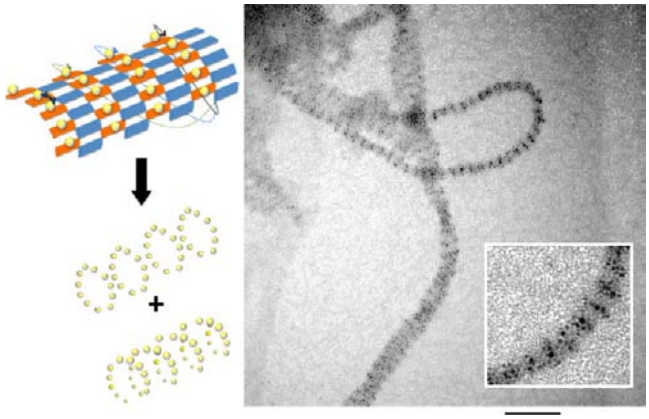

Figure 5. TEM micrograph from *in situ* reduction of Ag^+ onto arrays containing **bpdB1a**. (left) Schematic that shows how repulsions between metal NPs could lead to folding of flat arrays into tubes. The folding may occur with (green and blue dashed arrow) or without offset (black dashed arrow) leading to spiral or stacked arrays of NPs. The DNA array is omitted in the lower part of the figure for clarity. (right) Both types of metal arrays are seen in the micrograph. The inset shows a magnified image of rings of NPs in the stacked conformation.

formation of tubes with parallel stacked rings of NPs as well as spiral arrangements with either left- or right-handed helicity. The different types of tubes are produced as the rolling up can occur with or without any offset along the boundary that is being sealed during tube formation. Tubes with different diameters were also observed which reflects the starting widths of the flat sheets.

Interestingly the distance between the rows of AgNPs in the stacked ring conformation was measured to be 23 nm, which is lower than the expected value of 33 nm (also see Figure S10). Rothemund et al.[73] have shown that formation of tubes from these types of tiled arrays leads to a gentle bending of the helix spanning the intertile crossovers. It is possible that in the present case that the bending effect is exacerbated due to splitting of the B1 strand into two segments which could introduce a hinge site. The net effect of such an exaggerated bending motion would be to bring the rows of tiles (and NPs)

dx.doi.org/10.1021/ja400898s | *J. Am. Chem. Soc.* 2013, 135, 6234−6241

closer together. Irrespective of the possible reasons for the decreased spacing, these results clearly show the site-specific deposition of AgNPs by *in situ* reduction of Ag^+ by bpDNA.

In order to understand the effect of the number of borane groups (and therefore the reductive potential) on metal reduction, arrays containing the **3−1bpdB1a** were also treated with the $AgNO_3$ containing buffer described above. However in these arrays no metallization was observed. This was also true when higher concentrations of Ag^+ (up to 5 mM), longer incubation times (up to 3 days), or lower Mg^{2+} concentrations (1 mM) were used. These results are consistent with our previous finding[54] that a dithymidine boranephosphonate does not reduce silver at room temperature, but a fully boronated 21-mer oligothymidine reacts with Ag^+ ions to produce NPs. Thus a minimum number of borane groups in close proximity appears to be necessary in order to reduce enough silver ions to lead to formation of a stable seed particle at room temperature. When the Ag^+ treatment was carried out at a higher temperature (40 °C), uncontrolled metal deposition that resulted in ill-defined metal NP arrays was observed (Figure S12). In addition many unassociated NPs were also seen. These observations suggest that at higher temperatures the formation and growth of NPs do not occur solely on the arrays adhered to the surface. It is likely that unincorporated **3−1bpdB1a** containing tiles that are more mobile at higher temperature are responsible for this type of growth. In future experiments it would be instructive to use bpDNAs that contain different numbers of contiguous boranephosphonate linkages. Current efforts are directed toward using such oligomers within DNA nanoassemblies that assemble into discrete structures. These structures can be purified postassembly, which would remove artifacts that arise due to unincorporated bpDNA strands.

DISCUSSIONS

Here we have presented a method for *in situ* site-specific reduction of metals within a DNA assembly. This process was made possible by introducing a reductive group that is part of the DNA backbone. Unlike procedures that use presynthesized AuNPs, the resolution of the metallic features produced using bpDNA nanostructures is limited only by the underlying template. Moreover as the metal deposition step can be carried out *in situ*, the need for extra synthetic and purification steps required for AuNP conjugation to DNA oligomers is eliminated. Lower yields due to unwanted aggregation of DNA structures through binding of multiple assemblies to a single AuNP or through aggregation of the NPs[33,34] are also avoided.

A key development that enabled the use of bpDNA in DNA nanoassemblies was a new method for synthesizing bpDNA using 5′-DMT protected *N*-BIBS derivatives of dA, dG, and dC phosphoramidites. This represents the first reported use of a nucleobase protecting group that contains a N−Si bond during solid-phase 2′-deoxyoligonucleotide synthesis. The unique properties of these synthons (stability to bases and anhydrous acids as well a quantitative removal with mild fluoride treatment) make them ideally suited for synthesis of various base-sensitive DNA analogs.

CONCLUSIONS

We have introduced *N*-BIBS protected 2′-deoxynucleoside 3′-phosphosphoramidites as a new synthon that can be used to significantly extend our ability to synthesize boranephosphonate DNA. Subsequently we demonstrated the incorporation of these oligomers into 2D DNA arrays. *In situ* reduction of metal ions by bpDNA located at specific sites within these arrays demonstrated that specific patterns of AgNPs could be generated. Additionally bpDNA has been shown to possess properties useful for biological applications as antisense and antimir agents.[54] Thus the development of these methods for synthesizing bpDNA should stimulate more thorough investigations into their biological applications.

EXPERIMENTAL SECTION

Automated bpDNA Synthesis. Synthesis was carried out on an ABI 394 Synthesizer. All syntheses were performed at a 0.2 μmol scale using a 5′-DMT 2′-deoxythymidine joined to a low volume polystyrene solid support via a succinate linkage. In addition to **11**−**13**, 5′-dimethoxytrityl-2′-deoxythymidine-3′-*O*-methyl-*N*,*N*-diisopropylphosphoramidite (Glen Research) was used. For synthesis of 2′-deoxyoligonucleotides, a standard 0.2 μmole synthesis cycle was used with an increased coupling time of 120 s. A wash with methanol following the detritylation step was added. **11** and **12** and commercially obtained 5′-*O*-DMT-2′-deoxythymidine 3′-*O*-methyl *N*,*N*-diisopropylaminophosphoramidite (Glen Research) were dissolved in anhydrous CH_3CN, whereas **13** was dissolved in CH_2Cl_2 at a concentration of 0.1 M. Detritylation was carried out using a 0.5% solution of TFA in anhydrous $CHCl_3$ that also contained 10% TMPB. Solutions for boronation (0.05 M BH_3-THF complex in THF) and oxidation (1.0 M t-BuOOH in CH_2Cl_2) were prepared fresh prior to use. Reagents for activation (ethylthiotetrazole) and capping were purchased form Glen Research. A stepwise description of the synthesis cycle is described in Table S1.

Deprotection was carried out in two steps: The solid support linked 2′-deoxyoligonucleotides were first treated with a 1.0 M solution of disodium-2-carbamoyl-2-cyanoethylene-1,1-dithiolate in DMF for 1 h followed by extensive washing with DMF and methanol. The resin was then dried using a flow of argon. Subsequently these 2′-deoxyoligonucleotides were desilylated by overnight fluoride treatment (940 μL DMF + 470 μL Et_3N + 630 μL $Et_3N{\cdot}(HF)_3$). The resin was washed repeatedly with DMF, Millipore water, and methanol and dried with argon. The resin was then transferred to a glass vial and suspended in 37% ammonia for 1−2 h, and the ammoniawas removed by evaporation in a SpeedVac. The cleaved 2′-deoxyoligonucleotides were dissolved in a 10% acetonitrile-water mixture and used for further analysis and purification.

DNA Arrays. Preparation of DNA arrays was as described previously[10] except that the buffer was 20 mM tris-acetate (pH 7.6) containing 10 mM $Mg(OAc)_2$.

Atomic Force Microscopy. AFM images were obtained using the Cypher (Asylum Research) atomic force microscope. Silicon nitride levers with a nominal spring constant of 0.35 nm (Bruker) were used. DNA arrays were deposited on freshly cleaved mica by adding 3 μL of the array solution, waiting for 1−2 min and then adding 75 μL of buffer (20 mM tris-acetate (pH 7.6) + 10 mM $Mg(OAc)_2$). Imaging was carried out under liquid using the same buffer.

Metallization of bpDNA Containing Arrays. 400 mesh carbon-coated gold grids (Electron Microscopy Sciences) were cleaned by glow discharge immediately prior to use. The grids were first treated with a solution of 100 mM $Mg(OAc)_2$ for 5 min, the liquid was removed, and then the grids were washed with water. Next 2−4 μL of a solution containing the DNA arrays was added to the grid and allowed to stand for 10 min at room temperature. Subsequently the liquid was removed using a Kimwipe, and the grid washed once with water. At this stage 5 μL of the metallization solution (0.5 mM $AgNO_3$ + 10 mM $Mg(OAc)_2$ + 20 mM tris-acetate (pH 7.6)) was added on top of the grid, and the grid was incubated in a humidity chamber at room temperature for 20 h. For incubation of the grids at 40 °C, a procedure was developed in order to ensure that the liquid on the grids did not dry out. In this step the grids were floated onto 50 μL droplets of the metalizing solution that were put on top of a piece of

dx.doi.org/10.1021/ja400898s | J. Am. Chem. Soc. 2013, 135, 6234−6241

Teflon tape. The grids were then incubated in a humidity chamber that had been pre-equilibrated in an incubation oven set at 40 °C. Following incubation, the excess liquid was removed from the grid, and each grid was washed three times with 5 μL of water. The grids were allowed to air dry and TEM was carried out using a CM100 transmission electron microscope (FEI, Inc., Hillsboro, OR) operating at 80 kV.

■ ASSOCIATED CONTENT

Supporting Information

Detailed synthetic procedures, characterization data for compounds reported, HPLC and MALDI-TOF data for phosphate DNA sequences synthesized using BIBS-phosphoramidites as well as additional AFM and TEM images are provided. This information is available free of charge via the Internet at http://pubs.acs.org.

■ AUTHOR INFORMATION

Corresponding Author

marvin.caruthers@colorado.edu

Notes

The authors declare no competing financial interest.

■ ACKNOWLEDGMENTS

We would like to thank Prof. Thomas Perkins (CU, Boulder) and his laboratory members for generous use of their atomic force microscope, sharing their expertise in imaging techniques, and many helpful discussions. We also thank Prof Nadrian Seeman (NYU) for helpful discussions and suggestions throughout the project. This research was supported by the University of Colorado.

■ REFERENCES

(1) Maier, S. A.; Atwater, H. A. *J. Appl. Phys.* **2005**, *98*, 011101:1−011101:10.

(2) Willets, K. A.; Van Duyne, R. P. *Annu. Rev. Phys. Chem.* **2007**, *58*, 267−297.

(3) Seeman, N. C. *Annu. Rev. Biochem.* **2010**, *79*, 65−87.

(4) Samano, E. C.; Pilo-Pais, M.; Goldberg, S.; Vogen, B. N.; Finkelstein, G.; LaBean, T. H. *Soft Matter* **2011**, *7*, 3240−3245.

(5) Tan, S. J.; Campolongo, M. J.; Luo, D.; Cheng, W. *Nat. Nanotechnol.* **2011**, *6*, 268−276.

(6) Seeman, N. C. *Nature* **2003**, *421*, 427−431.

(7) Lin, C.; Liu, Y.; Rinker, S.; Yan, H. 2006, *7*, 1641−1647.

(8) Aldaye, F. A.; Palmer, A. L; Sleiman, H. F. *Science* **2008**, *321*, 1795−1799.

(9) Simmel, F. C. *Angew. Chem., Int. Ed.* **2008**, *47*, 5884−5887.

(10) Winfree, E.; Liu, F.; Wenzler, L. A.; Seeman, N. C. *Nature* **1998**, *394*, 539−544.

(11) Chen, J. H.; Seeman, N. C. *Nature* **1991**, *350*, 631−633.

(12) Yan, H.; Park, S. H.; Finkelstein, G.; Reif, J. H.; LaBean, T. H. *Science* **2003**, *301*, 1882−1884.

(13) Shih, M. W.; Quispe, J. D.; Joyce, G. F. *Nature* **2004**, *427*, 618−621.

(14) Rothemund, P. W. K.; Papadakis, N.; Winfree, E. *PLoS Biol.* **2004**, *2*, 2041−2053.

(15) Shih, M. W.; Quispe, J. D.; Joyce, G. F. *Nature* **2004**, *427*, 618−621.

(16) Rothemund, P. W. K. *Nature* **2006**, *440*, 297−302.

(17) He, Y.; Ye, T.; Su, M.; Zhang, C.; Ribbe, A. E.; Jiang, W.; Mao, C. *Nature* **2008**, *452*, 198−201.

(18) Yin, P.; Choi, H. M.; Calvert, C. R.; Pierce, N. A. *Nature* **2008**, *451*, 318−322.

(19) Yin, P.; Hariadi, R. F.; Sahu, S.; Choi, H. M. T.; Park, S. H.; LaBean, T. H.; Reif, J. H. *Science* **2008**, *321*, 824−826.

(20) Andersen, E. S.; Dong, M.; Nielsen, M. M.; Jahn, K.; Subramani, R.; Mamdouh, W.; Golas, M. M.; Sander, B.; Stark, H.; Oliveira, C. L. P.; Pedersen, J. S.; Birkedal, V.; Besenbacher, F.; Gothelf, K. V.; Kjems, J. *Nature* **2009**, *459*, 73−76.

(21) Douglas, S. M.; Dietz, H.; Liedl, T.; Hogberg, B.; Graf, F.; Shih, W. F. *Nature* **2009**, *459*, 414−418.

(22) Dietz, H.; Douglas, S. M.; Shih, W. M. *Science* **2009**, *325*, 725−730.

(23) Wei, B.; Dai, M.; Yin, P. *Nature* **2012**, *485*, 623−627.

(24) Braun, E.; Eichen; Sivan, U.; Ben-Yoseph, G. *Nature* **1998**, *391*, 775−778.

(25) Keren, K.; Krueger, M.; Gilad, R.; Benyoseph, G.; Sivan, U.; Braun, E. *Science* **2002**, *297*, 72−75.

(26) Yan, H.; Park, S. H.; Finkelstein, G.; Reif, J. H.; LaBean, T. H. *Science* **2003**, *301*, 1882−1884.

(27) Liu, D.; Park, S. H.; Reif, J. H.; Labean, T. H. *Proc. Natl. Acad. Sci. U.S.A.* **2004**, *101*, 717−722.

(28) Park, S. H.; Barish, R.; Li, H. Y.; Reif, J. H.; Finkelstein, G.; Yan, H.; LaBean, T. H. *Nano Lett.* **2005**, *5*, 693−696.

(29) Patolsky, F.; Weizmann, Y.; Lioubashevski, O.; Willner, I. *Angew. Chem., Int. Ed.* **2002**, *41*, 2323−2327.

(30) Aherne, D.; Satti, A.; Fitzmaurice, D. *Nanotechnology* **2007**, *18*, 125205.

(31) Ford, W. E.; Harnack, O.; Yasuda, A.; Wessels, J. M. *Adv. Mater.* **2001**, *13*, 1793−1797.

(32) Richter, J.; Mertig, M.; Pompe, W.; Monch, I.; Schackert, H. K. *Appl. Phys. Lett.* **2001**, *78*, 536−538.

(33) Geng, Y.; Liu, J.; Pound, E.; Gyawali, S.; Harb, J. N.; Woolley, A. T. *J. Mat. Chem* **2011**, *21*, 12126−12131.

(34) Becerril, H. A.; Ludtke, P.; Willardson, B. M.; Woolley, A. T. *Langmuir* **2006**, *22*, 10140−10144.

(35) Gu, Q.; Haynie, D. T. *Mater. Lett.* **2008**, *62*, 3047−3050.

(36) Gu, Q.; Haynie, D. T. *DNA-Templated Nanowires: Context, Fabrication, Properties and Applications In Annual Review of Nano-Research*; Cao, G., Brinker, C. J., Eds.; World Scientific Publishing Company, Inc.: Hackensack, NJ, 2008; Vol. *2*, pp 217−245.

(37) Keren, K.; Berman, R.; Braun, E. *Nano Lett.* **2004**, *4*, 323−326.

(38) Burley, G. A.; Gierlich, J.; Mofid, M. R.; Nir, H.; Tal, S.; Eichen, Y.; Carell, T. *J. Am. Chem. Soc.* **2006**, *128*, 1398−1399.

(39) Wirges, C. T.; Timper, J.; Fischler, M.; Sologubenko, A. S.; Mayer, J.; Simon, U.; Carell, T. *Angew. Chem., Int. Ed.* **2009**, *48*, 219−223.

(40) Alivisatos, A. P.; Johnsson, K. P.; Peng, X.; Wilson, T. E.; Loweth, C. J.; Bruchez, M. P., Jr; Schultz, P. G. *Nature* **1996**, *382*, 609−611.

(41) Sharma, J.; Chhabra, R.; Andersen, C. S.; Gothelf, K. V.; Yan, H.; Liu, Y. *J. Am. Chem. Soc.* **2008**, *130*, 7820−7821.

(42) Park, S. Y.; Lytton-Jean, A. K. R.; Lee, B.; Weigand, S.; Schatz, G. C.; Mirkin, C. *Nature* **2008**, *451*, 553−556.

(43) Sharma, J.; Chhabra, R.; Cheng, A.; Brownell, J.; Liu, Y.; Yan, H. *Science* **2009**, *323*, 112−116.

(44) Hung, A. M.; Micheel, C. M.; Bozano, L. D.; Osterbur, L. W.; Wallraff, G. M.; Cha, J. N. *Nat. Nanotechnol.* **2010**, *5*, 121−126.

(45) Ding, B.; Deng, Z.; Yan, H.; Cabrini, S.; Zuckerman, R. N.; Bokor, J. *J. Am. Chem. Soc.* **2010**, *132*, 3248−3249.

(46) Schreiber, R.; Kempter, S.; Holler, S.; Schuller, V.; Schiffels, D.; Simmel, S. S.; Nickels, P. C.; Liedl, T. *Small* **2011**, *7*, 1795−1799.

(47) Shen, X.; Song, C.; Wang, J.; Dangwei, S.; Wang, Z.; Liu, N.; Ding, B. *J. Am. Chem. Soc.* **2012**, *134*, 136−149.

(48) Pearson, A. C.; Liu, J.; Pound, E.; Uprety, B.; Woolley, A. T.; Davis, R. C.; Harb, J. N. *J. Phys. Chem. B* **2012**, *116*, 10551−10560.

(49) Pearson, A. C.; Pound, E.; Woolley, A. T.; Linford, M. R.; Harb, J. N.; Davis, R. C. *Nano Lett.* **2011**, *11*, 1981−1987.

(50) Pal, S.; Deng, Z.; Wang, H.; Zou, S.; Liu, Y.; Yan, H. *J. Am. Chem. Soc.* **2011**, *133*, 17606−17609.

(51) Kuzyk, A.; Schreiber, R.; Fan, Z.; Pardatscher, G.; Roller, E.; Hogele, A.; Simmel, F. C.; Govorov, A. O.; Liedl, T. *Nature* **2012**, *483*, 311−314.

(52) Pilo-Pais, M.; Goldberg, S.; Samano, E.; LaBean, T. H.; Finkelstein, G. *Nano Lett.* **2011**, *11*, 3489−3492.
(53) Sharma, J.; Chhabra, R.; Liu, Y.; Ke, Y.; Yan, H. *Angew. Chem., Int. Ed.* **2006**, *45*, 730−735.
(54) Roy, S.; Olesiak, M.; Padar, P.; McCuen, H.; Caruthers, M. H. *Org. Biomol. Chem.* **2012**, *10*, 9131−9134.
(55) Li, P.; Sergueeva, Z. A.; Dobrikov, M.; Shaw, B. R. *Chem. Rev.* **2007**, *107*, 4746−4796.
(56) Sood, A.; Shaw, B. R.; Spielvogel, B. F. *J. Am. Chem. Soc.* **1990**, *112*, 9000−9001.
(57) Tomasz, J.; Shaw, B. R.; Porter, K.; Spielvogel, B. F.; Sood, A. *Angew. Chem., Int. Ed.* **1992**, *31*, 1373−1375.
(58) Olesiak, M.; Krivenko, A.; Krishna, H.; Caruthers, M. H. *Phosphorus, Sulfur Silicon Relat. Elem.* **2011**, *186:4*, 921−932.
(59) Sergueev, D. S.; Shaw, B. R. *J. Am. Chem. Soc.* **1998**, *120*, 9417−9727.
(60) Higson, A. P.; Sierzchala, A.; Brummel, H.; Zhao, Z.; Caruthers, M. H. *Tet. Lett* **1998**, *39*, 3899−3902.
(61) Zhang, J.; Terhorst, T.; Matteucci, M. D. *Tet. Lett.* **1997**, *38*, 4957−4960.
(62) McCuen, H. B.; Noe, M. S.; Sierzchala, A. B.; Higson, A. P.; Caruthers, M. H. *J. Am. Chem. Soc.* **2006**, *128*, 8138−8139.
(63) Shimizu, M.; Saigo, K.; Wada, T. *J. Org. Chem.* **2006**, *71*, 4262−4269.
(64) Fu, T.-J.; Seeman, N. C. *Biochemistry* **1993**, *32*, 3211−3220.
(65) Virta, P. *ARKIVOC* **2009**, *iii*, 54−83.
(66) Liang, H.; Hu, L.; Corey, E. J. *Org. Lett.* **2011**, *13*, 4120−4123.
(67) Pratt, J. R.; Massey, W. D.; Pinkerton, F. H.; Thames, S. F. *J. Org. Chem.* **1975**, *40*, 1090−1094.
(68) Overman, L. E.; Okazaki, M. E.; Mishra, P. *Tet. Lett.* **1986**, *27*, 4391−4394.
(69) Paul, C. H.; Royappa, A. T. *Nucleic Acids Res.* **1996**, *24*, 3048−3052.
(70) Kawanaka, T.; Shimizu, M.; Shintani, N.; Wada, T. *Bioorg. Med. Chem. Lett.* **2008**, *18*, 3783−3786.
(71) Matsumura, F.; Oka, N.; Wada, T. *Org. Lett.* **2008**, *10*, 1557−1560.
(72) Castro, C. E.; Kilchherr, F.; Kim, D.; Shiao, E. L.; Wauer, P. W.; Bathe, M.; Dietz, H. *Nat. Methods* **2011**, *8*, 221−229.
(73) Rothemund, P. W. K.; Ekani-Nkodo, A.; Papadakis, N.; Kumar, A.; Fygenson, D. K.; Winfree, E. *J. Am. Chem. Soc.* **2004**, *126*, 16344−16352.